PLANAR BEAM-FORMING ARRAY FOR BROADBAND COMMUNICATION IN THE 60 GHZ BAND

J.A.G. Akkermans and M.H.A.J. Herben

Radiocommunications group,
Eindhoven University of Technology,
Eindhoven, The Netherlands,
e-mail: j.a.g.akkermans@tue.nl.

ABSTRACT

A planar beam-forming antenna array is proposed that operates in the 60 GHz frequency band. The array consists of 6 balanced-fed aperture-coupled patch antenna elements [2] that are placed in a circular configuration. The resulting array has a maximum gain of 14 dBi and a 3 dB scan range of ±50 degrees. To demonstrate the performance, test arrays have been implemented with accompanying feed networks that apply the appropriate phase distribution over the array for beam-forming at several specific scan angles. Measurements validate the proposed array configuration.

Key words: millimeter-wave antennas, planar array, beam-forming.

1. INTRODUCTION

Worldwide, there is an available bandwidth of 5 GHz in the frequency range from 59 to 64 GHz. Communication systems that operate in this license-free band have the potential to achieve data rates of multiple gigabits per second. Advances in semiconductor technology enable the use of low-cost Silicon-based electronics for these high frequencies. Therefore low-cost communications systems in the 60 GHz band can provide the next step in high data-rate wireless communication.

In order to achieve data rates of multiple gigabits per second, sufficient link budget is needed. Transceiver systems with directive antennas show a better performance in both line of sight and non line of sight conditions, since these configurations have better link margins and effectively suppress the multipath effect [5]. Still, the antenna beams of both the transmitter and the receiver should be aligned properly in order to utilise the advantages of directive antennas.

In this work, the design and realisation of a novel planar antenna array is presented that is suited for broadband wireless communication in the 60 GHz band. The antenna array is build-up out of balanced-fed aperture-coupled patch antennas, the design is presented in [2] and described shortly in Section 2. The antenna can be realised in printed circuit-board (PCB) technology, which results in a low-cost antenna solution. A circular array configuration with 6 antenna elements is proposed in Section 3. It is shown that this configuration minimises the mutual coupling between the elements and that it has a good performance in terms of antenna gain and antenna scan range. The antenna array supports beamforming, has a maximum directivity of 14 dBi and a 3 dB scan range of ±50 degrees. To demonstrate the performance of the beamforming, the array is implemented with different feed networks to obtain the required phase setting for beam-forming at different scan angles (Section 4).

2. ANTENNA ELEMENT

The geometry of the balanced-fed aperture-coupled antenna element is shown in Fig. 1. The antenna has a balanced coplanar microstrip feed to connect directly to a balanced power amplifier or balanced low-noise amplifier without the use of a balun. Two coupling apertures (slots) have been used to couple from the feed lines to the patch element. A reflector element is positioned at the back of the antenna to ensure a good front-to-back ratio. The resulting antenna design has dimensions which are less than $\lambda_0/2$, with λ_0 the free-space wavelength. Therefore the antenna can be used directly in array configurations. The antenna can be realised from two PCB boards with metallisation on both sides that are stacked with a prepreg layer in between.

The two slots have an important role in the antenna design. They are used to reduce the surface-wave excitation in the dielectric, and also to improve the antenna bandwidth. The slots are positioned such

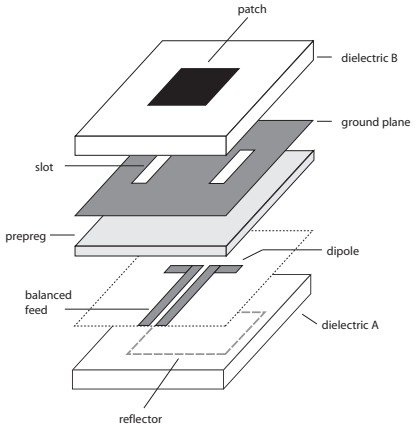

Figure 1. Geometry of the balanced-fed aperture-coupled patch with reflector element.

that the surface-waves that are generated by the slots and the patch interfere destructively. In conventional aperture-coupled patch designs, the slot is made small in terms of wavelengths such that the slot is non-resonant and the back radiation caused by it is reduced. In this design, the slots can be resonant in the operation band of the antenna because the reflector element compensates for the back radiation. As a result, the bandwidth is increased significantly since the antenna now has two resonant elements with slightly different resonance frequencies, i.e., the patch and both slots. An increase in bandwidth is observed from about 3% for the conventional single-element patch to more than 10% for the novel design.

The obvious thing to do would be to place the reflector element at a distance of $\lambda_d/4$, with λ_d the wavelength in the lower dielectric. However, this would significantly deteriorate the radiation efficiency because of the surface-wave excitation in the lower dielectric. Therefore, the thickness that has been chosen for the lower dielectric is equal to approximately $\lambda_d/20$. To reduce the back radiation, the size of the reflector element is adjusted accordingly [4].

The antenna element is optimised such that it has sufficient bandwidth to cover the frequency band from 57 to 64 GHz with a high radiation efficiency throughout this band [1]. The bandwidth of the antenna is more than 10% and the radiation efficiency is larger than 80% within the band of operation. The gain of the antenna is approximately 6 dBi.

3. PLANAR ARRAY

3.1. Hexagonal 7-element array

For the planar array there are two main configurations, which are related to the positions of the antenna elements. The antenna elements can be positioned in a square grid or in a hexagonal grid. For the square grid, the distance between the antenna elements should be less than half a free-space wavelength (λ_0) to avoid grating lobes. For the hexagonal grid, this is slightly different, since the distance between the phase centers of the elements should be less than $\lambda_0/2$. As a result the elements in the hexagonal grid can be placed at a distance which is less than $\lambda_0/\sqrt{3}$ (Fig. 2).

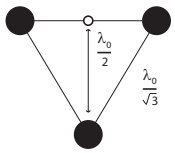

Figure 2. Inter-element distance of a hexagonal grid.

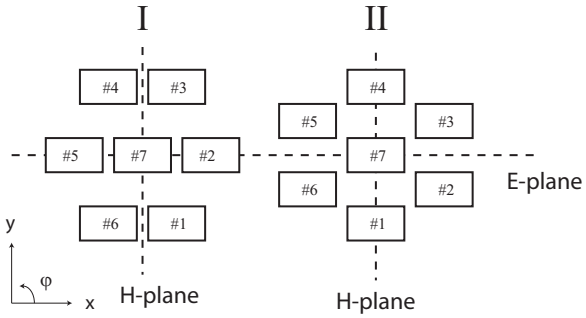

Figure 3. Two layouts for the 7-element hexagonal array.

The effect of mutual coupling on the performance of the antenna array can be quite significant. In general, the mutual coupling between elements decreases when the distance between the elements is increased. From this point of view, the hexagonal grid is a better choice. Another advantage of the hexagonal grid is that, compared to the square grid, the directivity of the array is larger for the same number of elements. This is because the effective aperture of the hexagonal array is larger than the effective aperture of the square array since the distance between the elements is larger for the hexagonal grid. The performance of the 7-element hexagonal array is investigated. Seven elements should be sufficient to acquire the desired antenna gain. Two possible layouts are shown in Fig. 3, where a rectangle is used to depict the approximate size of the antenna element. The radiation pattern of the antenna element is almost independent of azimuth angle φ. If mutual coupling between the elements is neglected, the performance of both layouts is equal. Still, both layouts show quite a different performance when the effect of mutual coupling is taken into account in a full-wave simulation.

The performance of the antenna array is modelled with a method-of-moments implementation which is

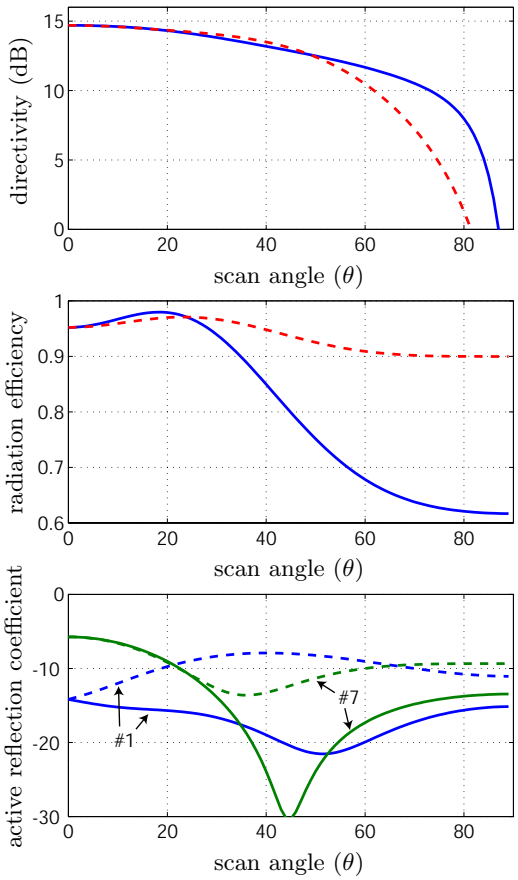

Figure 4. Hexagonal 7-element array, layout I. Directivity, radiation efficiency and active reflection coefficient for a scan in the $\varphi = 0°$ (solid lines) and $\varphi = 90°$ (dashed lines) plane. The active reflection coefficient is shown for a typical element and for the element with the worst performance.

based on the antenna model that is presented in [2]. An extension of this model is implemented such that finite antenna arrays consisting of balanced-fed aperture-coupled patch antenna elements can be analysed.

Figure 4 shows the directivity, radiation efficiency and active reflection coefficients as a function of elevation scan angle θ of array I in Fig. 3 for $\varphi = 0°$ (E-plane) and $\varphi = 90°$ (H-plane), respectively. The radiation efficiency η is defined as the ratio between radiated power in the whole upper hemisphere and accepted power at the antenna feed. The radiation efficiency of the single-element antenna is equal to about 80%. Most of the remaining 20% of power is excited into surface waves. In an array configuration, neighbouring elements excite surface waves that interfere and reduce or increase the total amount of surface-wave power depending on the phase distribution of the antenna elements. Therefore the radiation efficiency is a function of scan angle. The active reflection coefficient is an important parameter to analyse the behaviour of each antenna element under actual operation conditions, where each element is excited. The active reflection coefficient of element n is calculated as

$$\Gamma_n = 10 \log_{10} \left| \frac{Z^a_{\text{in},n} - Z_0}{Z^a_{\text{in},n} + Z_0} \right|^2 , \qquad (1)$$

here $Z^a_{\text{in},n}$ is the active input impedance and the characteristic impedance of the feed $Z_0 = 100\Omega$.

It is shown that the directivity as a function of scan angle are comparable in both planes. However, the difference in radiation efficiency is remarkable. This can be explained by examining the effect of the surface waves in the array configuration. The surface waves are excited mostly in the $\varphi = 0°$ direction. Therefore elements in this direction couple stronger than elements in the $\varphi = 90°$ direction. At broadside radiation, the elements are excited in phase and the inter-element distance is such that the surface waves are suppressed significantly. This results in a high radiation efficiency. When the beam is scanned in the $\varphi = 0°$ plane, the phases of the elements in this direction are adjusted accordingly. Since this affects the suppression of the surface waves, this introduces a significant impact on the radiation efficiency as well as on the active input impedance. A scan in the $\varphi = 90°$ plane will not affect the surface-wave suppression much, and therefore the radiation efficiency remains high for the entire scan range.

The active reflection coefficient should remain low for the whole scan range. In Fig. 4 it is observed that especially the centre element can have a high active reflection coefficient for some scan angles. This is undesired, since it introduces additional reflection losses in the transceiver system.

The performance of layout I can be improved by changing to layout II. In this layout the inter-element distance is as large as possible in the $\varphi = 0°$ plane. Therefore the elements couple less and the performance of the array is more symmetric in both planes (Fig. 5). Also the active reflection coefficient shows some better performance because of the reduced coupling between the elements.

3.2. Circular 6-element array

To reduce the mutual coupling within the array, the middle element in layout II of the hexagonal 7-element array is removed. This results in a circular 6-element array. The performance of the circular array is shown in Fig. 6 and it is observed that this performance is superior to the performance of the hexagonal array although only 6 elements are used. The reason for this is that the aperture area of the antenna array remains the same while the mutual coupling within the array is reduced. Because the array has no center element, the aperture area

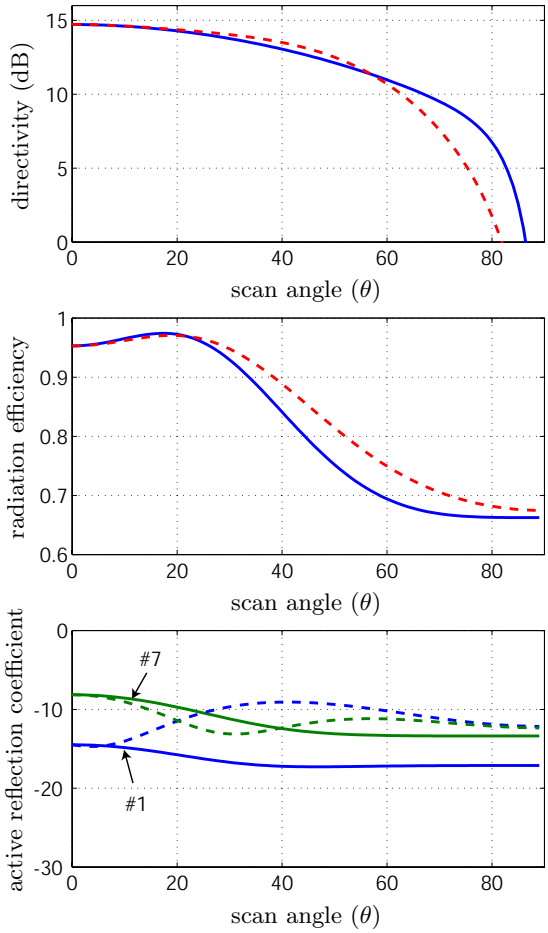

Figure 5. Hexagonal 7-element array, layout II. Directivity, radiation efficiency and active reflection coefficient for a scan in the $\varphi = 0°$ (solid lines) and $\varphi = 90°$ (dashed lines) plane. The active reflection coefficient is shown for a typical element and for the element with the worst performance.

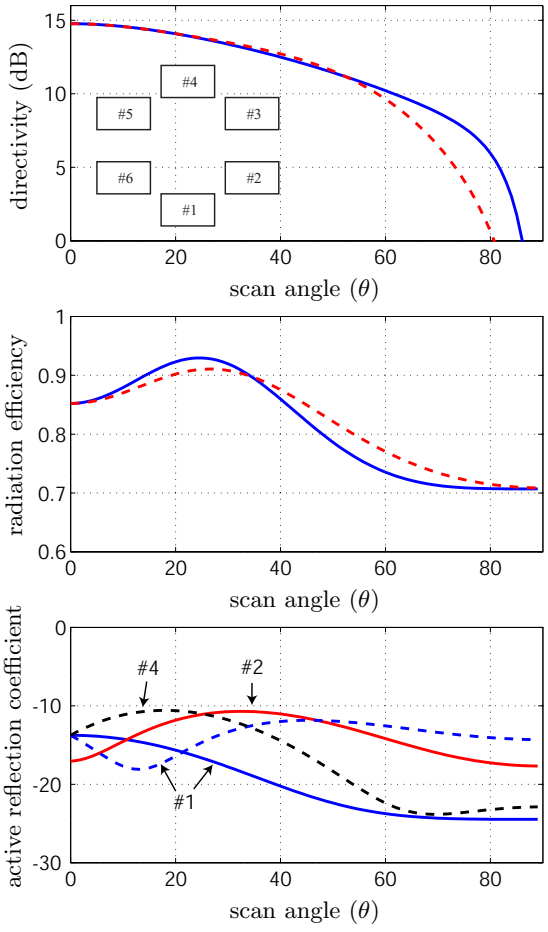

Figure 6. Circular 6-element array. Directivity, radiation efficiency and active reflection coefficient for a scan in the $\varphi = 0°$ (solid lines) and $\varphi = 90°$ (dashed lines) plane. The active reflection coefficient is shown for a typical element and for the element with the worst performance.

is not illuminated homogenously. Therefore a slight decrease in directivity is observed for larger scan angles compared to the 7-element array. However, the advantage is that the active reflection coefficient remains below -10 dB throughout the whole scan range for each antenna element.

4. BEAM-FORMING

The antenna array will be used in a transceiver system in which each antenna element will have its own balanced phase shifter, power amplifier and low-noise amplifier implemented on a separate integrated circuit close to the antenna element. At this moment, this circuitry is not available yet. Therefore, the capabilities of beam-forming with the circular array is demonstrated by using separate feed networks that provide each antenna element with the correct phase for a specific fixed scan angle.

The circular antenna array and accompanying feed network for beam-forming is shown in Fig. 7. Here, the feed network is designed such that the main lobe points to $\theta = 30°$ and $\phi = 0°$. Each antenna element is connected to a balun and the antenna elements are combined using a Bagley power divider in combination with a Wilkinson power divider. The antenna is connected with an RF probe which is landed on a coplanar waveguide transmission line. A transition from coplanar waveguide to microstrip is designed to facilitate the interconnection with the feed network [3].

Feed networks have been designed for scan angles in the E-plane, H-plane and diagional (D) plane. The scan angles that have been selected in each plane are 0, 30, 45 and 60 degrees. The performance of each antenna board is verified with the developed MoM model and a full-wave finite-volume simulation tool (CST Microwave Studio). The effect of the feed network and the effect of the diffraction at the edges

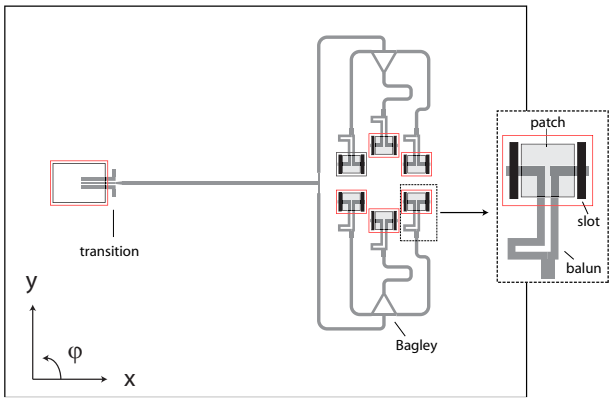

Figure 7. Layout of the circular 6-element array with beam-forming network for 30° scan in $\varphi = 0°$ plane. Inset: geometry of the antenna element and balun.

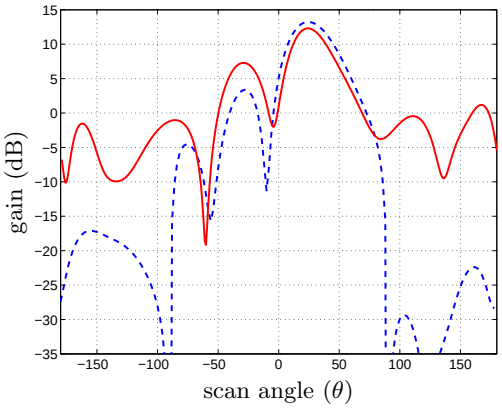

Figure 8. Gain of circular array for $\theta = 30°$ scan in the $\varphi = 0°$ plane. CST (solid), MoM model (dashed).

of the board is not accounted for in our MoM model, whereas CST Microwave Studio can incorporate all these effects. In Fig. 8, the difference in radiation pattern between the two models is observed. Both models predict a similar main lobe, but CST predicts a higher side lobe level due to the diffraction at the edges of the board and more back radiation due to the radiation of the feed network.

5. MEASUREMENTS

To validate the antenna designs, the antenna has been manufactured in PCB technology. The dielectric for the antenna is Neltec NY9217, which has a dielectric constant of 2.17, specified at 10 GHz. SpeedBoard C has been used as prepreg. It has a dielectric constant of 2.6, specified up to 40 GHz. These materials are the same materials that have been used for the single-element antenna design [2]. The thickness of the upper and lower dielectric board is chosen as 254 μm and the thickness of the prepreg layer equals 112 μm.

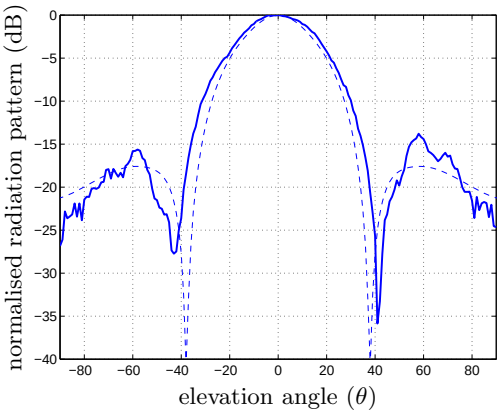

Figure 9. Normalised H-plane radiation pattern of the circular array at broadside scan ($\theta = 0°$). Frequency = 60 GHz. Measurement (solid), simulation (dashed).

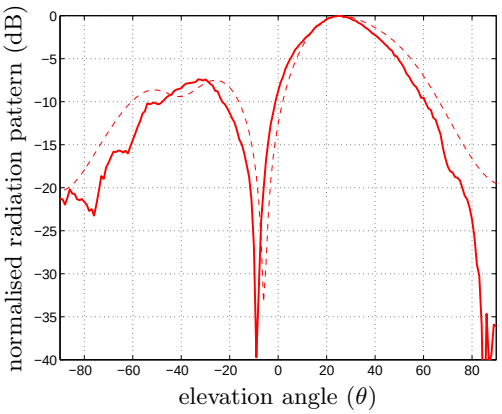

Figure 10. Normalised H-plane radiation pattern of the circular array at $\theta = 30°$ scan. Frequency = 60 GHz. Measurement (solid), simulation (dashed).

The radiation patterns of the antennas have been measured with a far-field measurement setup that is described in [3]. This setup can connect to the antenna with an RF probe and is able to measure the far-field radiation pattern of the antenna under test in the upper hemisphere. The radiation patterns of the circular antenna arrays that scan in the H-plane at $\theta = 0°, 30°, 60°$ are shown in Figs. 9-11. It is shown that the antenna arrays are able to scan up to $\theta = 60$ degrees in the H-plane and that the radiation patterns are in agreement with simulation. Similar performance is observed for scanning in the E-plane and D-plane.

6. CONCLUSIONS

A low-cost planar beam-forming array configuration is presented that operates in the 60 GHz band. The array is implemented in low-cost PCB technology. A circular configuration is proposed that minimises the mutual coupling within the array. The scan perfor-

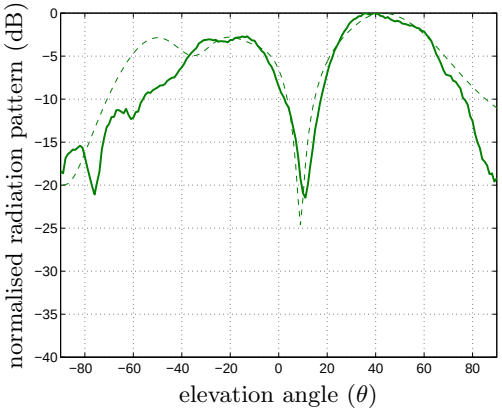

Figure 11. Normalised H-plane radiation pattern of the circular array at $\theta = 60^\circ$ scan. Frequency = 60 GHz. Measurement (solid), simulation (dashed).

mance of the array is modelled and investigated. The capabilities of beam-forming with the circular array is demonstrated by using separate feed networks that provide each antenna element with the correct phase for specific scan angles. The radiation patterns have been measured and it is shown that they are in agreement with simulation results.

ACKNOWLEDGEMENTS

The authors would like to thank Marcel van der Graaf and Raymond van Dijk for their help in the measurement of the antenna characteristics at the laboratory of TNO Defence and Security in The Hague, The Netherlands.

REFERENCES

1. J.A.G. Akkermans and M.H.A.J. Herben. Sensitivity analysis and optimisation of electromagnetic structures. In *EMTS International Symposium on Electromagnetic Theory*, pages 1–3, July 2007.

2. J.A.G. Akkermans, M.C. van Beurden, and M.H.A.J. Herben. Design of a millimeter-wave balanced-fed aperture-coupled patch antenna. In *proc. EuCAP 2006, ESA SP626*, Nice, France, November 2006.

3. J.A.G. Akkermans, R. van Dijk, and M.H.A.J. Herben. Millimeter-wave antenna measurement. In *EuMC European Microwave Conference*, pages 1–4, October 2007.

4. S.D. Targonski and R.B. Waterhouse. Reflector elements for aperture and aperture coupled microstrip antennas. In *Antennas and Propagation Society International Symposium*, volume 3, pages 1840–1843. IEEE, July 1997.

5. H. Yang, P.F.M. Smulders, and M.H.A.J. Herben. Channel characteristics and transmission performance for various channel configurations at 60 GHz. *EURASIP Journal on Wireless Communications and Networking*, 2007:1–15, 2007.